Journal of Organometallic Chemistry, 443 (1993) 199–206

JOM 23041

The redox behaviour of ferrocene derivatives

I. 1,2,3-Tritellura[3]ferrocenophane and 1,3-ditellura[3]ferrocenophanes

Piero Zanello and Giuliana Opromolla

Dipartimento di Chimica dell'Università di Siena, Pian dei Mantellini, 44, 53100 Siena (Italy)

Maurizio Casarin

Dipartimento di Chimica Inorganica, Metallorganica ed Analitica dell'Università, Via Loredan 4, 35131 Padova (Italy)

Max Herberhold and Peter Leitner

Laboratorium für Anorganische Chemie der Universität, Postfach 10 12 51, W-8580 Bayreuth (Germany)

(Received May 6, 1992)

Abstract

The electrochemical behaviour of 1,2,3-tritellura[3]ferrocenophane, $[Fe(C_5H_4Te)_2Te]$, and 1,3-ditellura[3]ferrocenophanes, $[Fe(C_5H_4Te)_2E']$ (E' = S, Se, or CH_2), has been examined and compared to that of the known tri- and di-chalcogena[3]ferrocenophanes. All the complexes undergo a chemically reversible one-electron oxidation. 1,2,3-Tritellura[3]ferrocenophane also exhibits a clean reduction step, even if complicated by subsequent chemical reactions. Discrete variational (DV-Xα) calculations relative to the model compounds $[Fe(C_5H_4Te)_2Te]$, $[Fe(C_5H_4Se)_2Se]$, and $[Fe(C_5H_4S)_2S]$ allow an unambiguous assignment of the molecular orbitals involved in the oxidation and reduction processes. They suggest that the all-tellura[3]ferrocenophane complex, $[Fe(C_5H_4Te)_2Te]$, is the most accessible both to one-electron addition and removal steps.

1. Introduction

Trichalcogena[3]ferrocenophanes, $[Fe(C_5H_4E)_2E']$, are interesting compounds both with respect to their molecular geometry in the solid state and to their fluxional behaviour in solution. The [3]ferrocenophanes containing sulfur and selenium directly attached to the cyclopentadienyl rings (E = S or Se) have been extensively studied since 1969, when 1,2,3-trithia[3]ferrocenophane, $[Fe(C_5H_4S)_2S]$ (**1a**), was first reported by Davison and Smart [1]. However, the corresponding tellurium compounds (E = Te) were obtained only recently following the preparation of 1,2,3-tritellura[3]ferrocenophane, $[Fe(C_5H_4Te)_2Te]$ (**3c**) [2,3].

Correspondence to: Professor P. Zanello or Professor M. Herberhold.

At the present time, all nine possible 1,2,3-trichalcogena[3]ferrocenophanes $[Fe(C_5H_4E)_2E']$ (**1a–1c**, **2a–2c**, and **3a–3c**), are available for physicochemical studies [3].

The all-tellura[3]ferrocenophane $[Fe(C_5H_4Te)_2Te]$ (**3c**), possesses the expected molecular structure with nearly parallel and almost eclipsed cyclopentadienyl rings [2]. Compared with the analogous compounds $[Fe(C_5H_4S)_2S]$ (**1a**) [4], $[Fe(C_5H_4S)_2Se]$ (**1b**) [5], $[Fe(C_5H_4Se)_2Se]$ (**2b**) [6] and $[Ru(C_5H_4Se)_2Se]$ [7], the larger tellurium atoms in **3c** cause small deviations from the ideal geometry [2]. Thus, the ring canting and the outwards displacement of the chalcogens E from the plane of their cyclopentadienyl ring are slightly larger in **3c**, whereas the angle at the central tellurium atom (91.6(1)° and 93. 9(1)° for the two molecules of the asymmetric unit) [2] is significantly smaller than the analogous angle in the comparable ferrocenophanes **1a**

0022-328X/93/$6.00

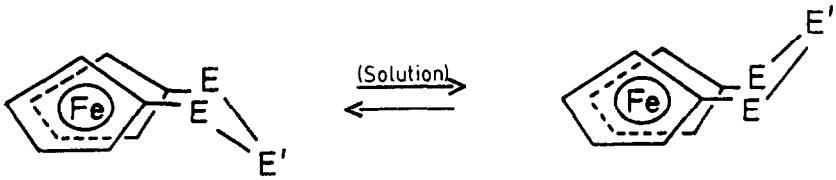

E = S E = Se E = Te

E' = S (1a) E' = S (2a) E' = S (3a)
Se (1b) Se (2b) Se (3b)
Te (1c) Te (2c) Te (3c)
CH_2 (1d) CH_2 (2d) CH_2 (3d)

(103.9(2)°) [4], **1b** (100.5(1)°) [5] and **2b** (100.7°) [6].

In solution the all-tellura[3]ferrocenophane (**3c**) undergoes bridge-reversal more easily than any other 1,2,3-trichalcogena[3]ferrocenophane. The ^1H and ^{13}C nuclear magnetic resonance (NMR) solution spectra of all nine trichalcogena[3]ferrocenophanes (**1a–1c**, **2a–2c**, and **3a–3c**) are temperature-dependent, indicating non-rigidity in solution above room temperature [8,9]. The energy barrier of the bridge-reversal depends on the size of the intramolecular trichalcogen chain; the highest free activation enthalpy, ΔG^* (298 K), is observed for $[Fe(C_5H_4S)_2S]$ (**1a**) (80.4 ± 0.2 kJ mol^{-1}) [8], whereas $[Fe(C_5H_4Se)_2Se]$ (**2b**) (67.2 ± 0.1 kJ mol^{-1}) [8] is more flexible and the smallest barrier is found for $[Fe(C_5H_4Te)_2Te]$ (**3c**) (51.8 ± 0.2 kJ mol^{-1}) [9]. According to CNDO/2 calculations, the bridge inversion process probably proceeds through a transition state with staggered cyclopentadienyl rings rather than through a transition structure with eclipsed cyclopentadienyl rings and a trichalcogen bridge which is coplanar with the iron atom [9].

We assumed that 1,2,3-tritellura[3]ferrocenophane, $[Fe(C_5H_4Te)_2Te]$ (**3c**), might also be exceptional in its redox behaviour. The electrochemistry of a number of 1,2,3-trichalcogena[3]ferrocenophanes, $Fe(C_5H_4E)_2E'$ (E = S or Se) has been studied [10–12]. We now present a complementary investigation of the redox behaviour of the tellurium compounds, **3a–3d**.

2. Results and discussion

2.1. Electrochemistry of 1,2,3-tritellura[3]ferrocenophane, $[Fe(C_5H_4Te)_2Te]$

Figure 1(a) shows the redox behaviour of $[Fe(C_5H_4Te)_2Te]$ (**3c**) in dichloromethane solution.

Peaks A and D are typical of a simple redox couple. However, the second oxidation peak B and the cathodic peak E show, in the reverse scan, associated signals which are indicative of complicated redox changes.

The simple first oxidation step is clear from the cyclic voltammogram at low scan rate (Fig. 1(b)). In addition, controlled potential coulometry at $E_w = 0.7$ V consumes one-electron per molecule as the originally red–brown solution becomes reddish. The one-electron oxidized solution exhibits a cyclic voltammogram complementary to that illustrated in Fig. 1(b). Unexpectedly, paramagnetic resonance polycrystalline [Fe-

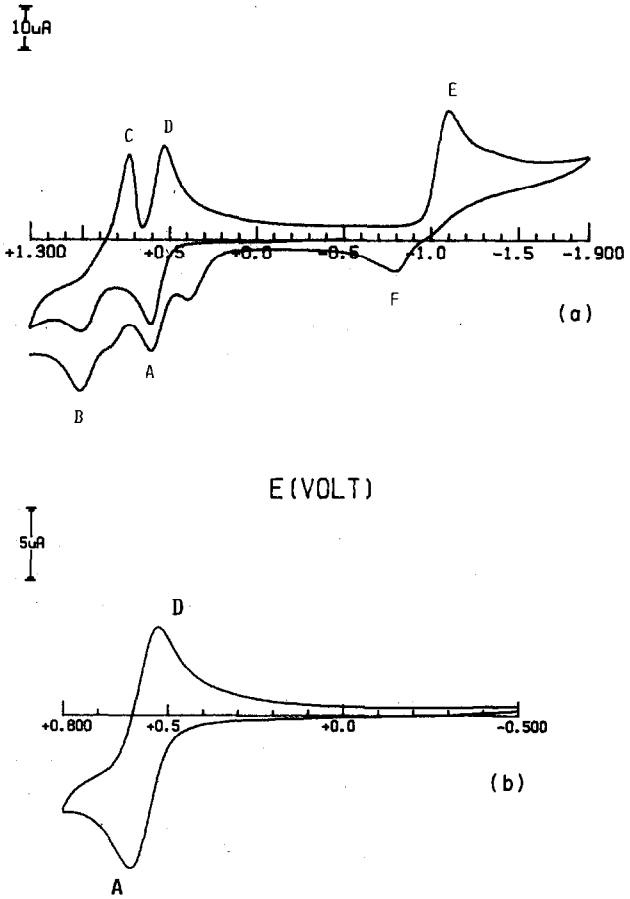

Fig. 1. Cyclic voltammograms recorded at a platinum electrode on a CH_2Cl_2 solution containing $[Fe(C_5H_4Te)_2Te]$ (**3c**) (1.2×10^{-3} mol dm^{-3}) and $[NBu_4][ClO_4]$ (0.2 mol dm^{-3}). Scan rate: (a) 0.2 V s^{-1}; (b) 0.05 V s^{-1}.

$(C_5H_4Te)_2Te]^+$ is electron silent even at 4 K. We have no straightforward explanation for this except for unusually fast relaxation processes.

Cyclic voltammograms of the peak system A/D with the scan rate v varying from 0.02 V/s^{-1} to 2.00 V/s^{-1} confirm that it is involves a simple reversible one-electron redox change [13]. (i) The peak–current ratio ip_D/ip_A is constant and unity; (ii), the peak-to-peak separation, ΔE_p, progressively increases from 72 mV to 164 mV and (iii), the current function $ip_A/v^{1/2}$ remains essentially constant.

The variation in ΔE_p with scan rate, in the absence of structural information on the ferrocenium cation $[Fe(C_5H_4Te)_2Te]^+$, allows us to estimate the extent of stereochemical reorganization accompanying the one-electron oxidation $Fe(C_5H_4Te)_2Te/[Fe(C_5H_4Te)_2Te]^+$. We have often compared it with the peak-to-peak separation of the anodic response of ferrocene [14], but we now think comparison with the oxidation of decamethylferrocene to be more appropriate. Although the variations in bond lengths accompanying the oxidation of unsubstituted ferrocene are firmly established, the relevant conformational changes are not [15]. In decamethylferrocene, it appears that oxidation is accompanied by an increase of 0.06 Å of the Fe-ring centroid distance (from 1.656 Å to 1.715 Å), and a concomitant rearrangement of the cyclopentadienyl rings from the staggered (D_{5d}) to the eclipsed (D_{5h}) conformation [16].

We observe that, under the experimental conditions described here for the oxidation of **3c**, the peak-to-peak separation relevant to the one-electron oxidation of $[Fe(C_5Me_5)_2]$ ($E^{o\prime} = +0.34$ V) increases from 72 mV to 173 mV. Assuming that the solvation processes of the two redox couples are similar, this would suggest that the barriers to structural rearrangement accompa-

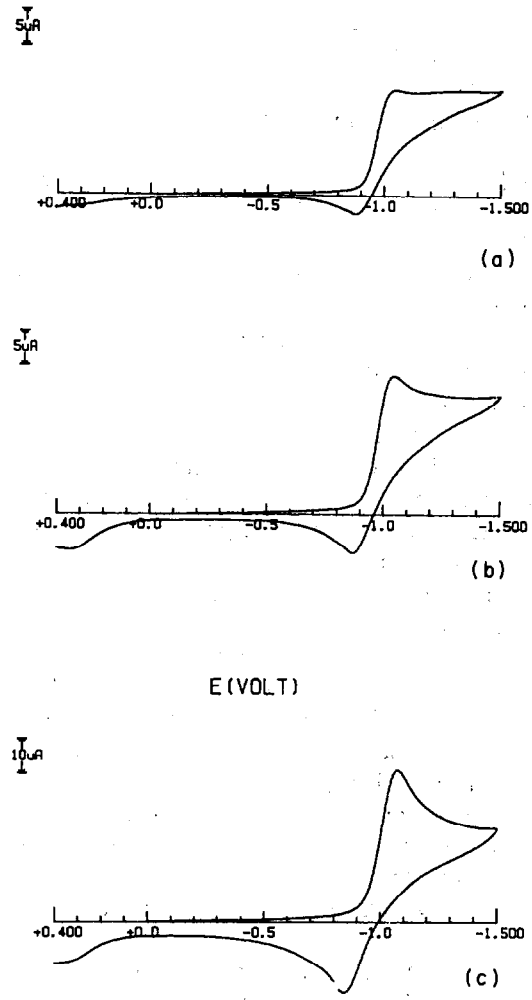

Fig. 2. Cyclic voltammograms recorded at a platinum electrode on a CH_2Cl_2 solution containing $[Fe(C_5H_4Te)_2Te]$ (**3c**) (1.2×10^{-3} mol dm^{-3}) and $[NBu_4][ClO_4]$ (0.2 mol dm^{-3}). Scan rate: (a) 0.05 V s^{-1}; (b) 0.1 V s^{-1}; (c) 0.5 V s^{-1}.

TABLE 1. Self-consistent-multipolar discrete variational atomic character for $Fe(C_5H_4S)_2S$ (**1a**)

MO	Eigenvalue $-\epsilon$ (eV)	Population (%)										Character
		Fe			2S			μ-S			$(C_5H_4)_2$	
		s	p	d	s	p	d	s	p	d		
22a′	0.47	0	0	5	5	27	8	10	32	3	10	
18a″	0.61	0	0	46	0	1	1	0	1	0	51	
17a″	0.73	0	0	43	1	4	2	0	3	0	47	
21a′ [a]	3.50	0	0	65	0	10	0	1	7	0	17	Fe d_{xz}
20a′	3.62	0	0	82	0	1	0	0	2	0	15	Fe d_{z^2}
19a′	3.84	0	0	80	0	3	0	0	1	0	16	Fe $d_{x^2-y^2}$
18a′	4.07	0	0	22	1	33	1	3	28	1	11	
16a″	4.47	0	0	8	0	78	0	0	0	1	13	S n^-
17a′	5.34	0	2	0	0	13	0	2	22	0	61	
16a′	5.51	0	1	0	0	7	0	1	4	0	87	
15a′	5.72	0	1	1	2	20	1	2	31	0	42	
15a″	6.05	0	0	30	0	0	0	0	0	0	70	πCp → Fe_{yz}
14a″	6.31	0	2	25	2	10	0	2	0	0	69	πCp → Fe_{xy}

[a] Highest occupied MO.

nying the redox changes are similar. The bridge reversal motion of **3c** in solution may involve a transition state having staggered cyclopentadienyl rings [9]. However, it must also be recognised that the interannular trichalcogen bridge in [3]ferrocenophanes probably tends to prevent the rotation of the cyclopentadienyl rings possibly induced by the one-electron removal, while favouring their tilting from the strictly parallel position [17].

Figure 2 shows the cathodic response of **3c** at different scan rates.

The steady-state current observed at slow scan rates is diagnostic of a catalytic process regenerating the starting compound [13]. On the short cyclic voltammetry time scale, increase of scan rate increasingly prevents such a chemical complication; concomitantly, the current function $ip/v^{1/2}$ decreases significantly. On the longer time scale of controlled potential electrolysis ($E_w = -1.3$ V), more than four electrons/molecule are consumed. After exhaustive reduction no trace of the $[Fe(C_5H_4Te)_2Te]/[Fe(C_5H_4Te)_2Te]^+$ couple is detectable. This suggests that decomposition reactions also parallel the chemical regeneration **3c**. To a first approximation, we attribute the main chemical complication to a simple disproportionation of the transient iron(I) anion $[Fe(C_5H_4Te)_2Te]^-$, which is instantaneously electrogenerated. Exhaustive reduction of **3c** might lead to reductive cleavage of the tritellurium bridge eventually to give the anions Te^{2-} and $[Fe(C_5H_4Te)_2]^{2-}$, which then undergo further reactions.

As far as the second anodic process illustrated in Fig. 1 is concerned, we did not carry out further investigations, because controlled potential coulometry ($E_w = +1.1$ V) indicated the occurrence of electrode poisoning phenomena.

In conclusion, the overall redox processes exhibited by **3c** can be summarized schematically as follows:

$$[Fe(C_5H_4Te)_2Te]^{2+} \longrightarrow \text{decomposition products}$$

$$Ep = +1.00\ V \quad \uparrow -e$$

$$[Fe(C_5H_4Te)_2Te]^{+}$$

$$E^{o\prime} = +0.57\ V \quad +e \Big\uparrow -e$$

$$[Fe(C_5H_4Te)_2Te]\ (\mathbf{3c})$$

$$E^{o\prime} = -0.96\ V \quad +e \Big\downarrow -e$$

$$[Fe(C_5H_4Te)_2Te]^{-} \longrightarrow \text{decomposition products}$$

The observation that ferrocene molecules are able to add one electron is not unusual, but the reduction usually occurs at very negative potential and can be detected only at low temperatures (less than −30°C) [18]. In an attempt to interpret the relatively easy reduction of **3c**, a theoretical comparative study of the 1,2,3-trichalcogena[3]ferrocenophanes $[Fe(C_5H_4E)E']$ {E = E′ = S (**1a**), Se (**2b**), Te (**3c**)} was carried out (see below). The smallest HOMO–LUMO separation was found for $[Fe(C_5H_4Te)_2Te]$ (**3c**). This could explain the actual access to both one-electron addition and one-

TABLE 2. Self-consistent-multipolar discrete variational atomic character for $Fe(C_5H_4Se)_2Se$ (**2b**)

MO	Eigenvalue $-\epsilon$ (eV)	Population (%)										Character
		Fe			2Se			μ-Se			$(C_5H_4)_2$	
		s	p	d	s	p	d	s	p	d		
22a′	0.98	−1	0	3	4	40	4	7	35	1	7	
18a″	1.00	0	0	46	0	1	0	0	0	0	53	
17a″	1.08	0	0	30	3	17	1	0	13	1	36	
21a′ [a]	3.73	0	0	44	0	24	0	1	16	0	15	
20a′	3.94	0	0	79	0	1	0	0	3	0	17	Fe d_{z^2}
16a″	4.02	0	0	5	0	86	0	0	0	0	9	Se n^-
19a′	4.08	−1	0	64	0	8	0	0	14	0	15	Fe($d_{x^2-y^2} + d_{xz}$)
18a′	4.16	0	0	61	0	14	0	1	10	0	14	Fe($d_{z^2} + d_{x^2-y^2} + d_{xz}$)
17a′	5.13	0	0	2	0	43	0	2	43	0	10	
16a′	5.67	0	0	1	3	5	0	1	18	0	72	
15a′	5.86	0	1	0	0	0	0	0	1	0	98	
15a″	6.35	0	0	29	0	1	0	0	0	0	70	πCp → Fe d_{yz}
14a″	6.43	0	0	26	0	6	0	0	2	0	66	πCp → Fe d_{xy}

[a] Highest occupied MO.

TABLE 3. Self-consistent-multipolar discrete variational atomic character for $Fe(C_5H_4Te)_2Te$ (3c)

MO	Eigenvalue $-\epsilon$ (eV)	Population (%)												Character
		Fe			2Te				μ-Te				$(C_5H_4)_2$	
		s	p	d	s	p	d	f	s	p	d	f		
22a′	0.41	0	0	3	4	45	5	0	7	29	1	0	6	
18a″	0.50	0	0	44	0	0	0	0	0	0	0	0	66	
17a″	0.80	0	0	12	3	10	3	0	0	28	3	0	41	
16a″ [a]	3.20	0	0	5	0	89	0	0	0	0	0	0	6	Te n^-
21a′	3.34	0	1	42	0	27	1	0	1	15	0	0	13	
20a′	3.52	0	0	72	0	3	0	0	0	9	0	0	16	$Fe(d_{z^2} + d_{x^2-y^2})$
19a′	3.62	−1	0	73	0	3	0	0	0	8	0	0	17	$Fe(d_{z^2} + d_{xz} + d_{x^2-y^2})$
18a′	3.74	0	0	57	0	17	0	0	1	12	0	0	13	$Fe(d_{z^2} + d_{xz} + d_{x^2-y^2})$
17a′	4.38	0	0	5	0	39	1	0	1	46	1	0	7	
16a′	5.17	0	1	0	3	10	0	0	1	22	0	0	63	
15a′	5.38	0	1	0	0	1	0	0	0	1	0	0	97	
15a″	5.81	0	0	11	4	30	0	0	0	3	0	0	52	$\pi Cp \rightarrow Fe\ d_{yz}$
14a″	5.84	0	0	22	3	14	0	0	0	10	0	0	51	$\pi Cp \rightarrow Fe\ d_{xy}$

[a] Highest occupied MO.

electron removal, which was not observed previously for **1a** and **2b**, [10–12].

2.2. *Theoretical study of the 1,2,3-trichalcogena[3]ferrocenophanes, $[Fe(C_5H_4E)_2E']$ (E = E′ = S, Se or Te)*

The electronic structure of **1a**, **2b**, and **3c** can be conveniently described in relation to $[Fe(\eta^5 - C_5H_5)_2]$, the bonding scheme of which has been thoroughly investigated both experimentally and theoretically [19–24]. It has been shown that the highest occupied MOs of ferrocene are strongly localized on the iron atom (e_2' and a_1', assuming an eclipsed conformation for the two cyclopentadienyl rings D_{5h} symmetry), the e_2' pair being weakly Fe–Cp bonding, whereas the a_1' MO is essentially non-bonding. Trivial symmetry considerations as well as qualitative arguments lead us to suppose that the main features of the electronic structure of $[Fe(C_5H_5)_2]$ should be maintained in the [3]ferrocenophanes. However, the presence of the high lying chalcogenide lone pairs must be taken into account.

The eigenvalues as well as the Mulliken [25] charge density analyses of the outermost MOs of **1a**, **2b**, and **3c** are given in Tables 1–3.

The quantitative theoretical results completely confirm the qualitative analysis. In **1a** the three outermost orbitals (21a′, 20a′, 19a′ MOs in Table 1) are reminiscent of the metal-based $e_2' + a_1'$ levels of ferrocene (which are localized on the 3d-Fe AOs and the C_5H_4 fragments). Moreover, the two lowest unoccupied orbitals 17a″ and 18a″ are the metal-based antibonding partners of the 15a″ and 14a″ MOs responsible for the Cp $\pi \rightarrow$ Fe $3d_{yz}$ and Cp $\pi \rightarrow$ Fe $3d_{xy}$ transitions,

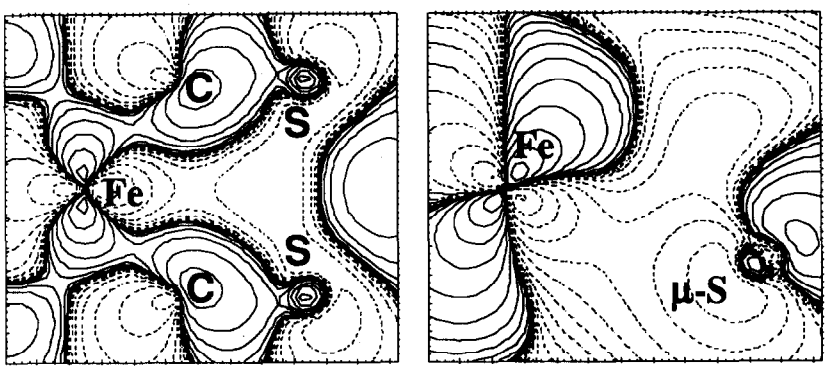

MO 18a′ in the XY Plane (a)

MO 18a′ in the XZ Plane (b)

Fig. 3. DV-X α contour plots of the 18a′ MO: (a) in the *XY* plane; (b) in the *XZ* plane. Logarithmic contour levels are $\pm 8 \times 10^{-4}$; $\pm 16 \times 10^{-4}$; $\pm 32 \times 10^{-4} \ldots e^{1/2}$ Å$^{-3/2}$.

respectively. Particularly interesting is the behaviour of the 18a′ and 16a″ MOs along the series. As illustrated in Fig. 3, the former is strongly delocalized in $[Fe(C_5H_4S)_2S]$ (**1a**), is antibonding with respect to the Fe–Cp interaction (Fig. 3(a)) and, at the same time, accounts for a long-range bonding interaction between the central sulfur atom (E′ = S) and the metallic centre (Fig. 3(b)).

As shown in Fig. 4, the MO 16a″ represents the antisymmetric combination of S lone pairs, roughly perpendicular to the C–S–S′ bridge.

On moving from $[Fe(C_5H_4S)_2S]$ (**1a**) to $[Fe(C_5H_4Te)_2Te]$ (**3c**), the energy levels of the MOs strongly localized on Fe (21a′, 20a′, 19a′ MOs in **1a**, 20a′, 19a′, 18a′ MOs in **2b** and **3c**) are only slightly affected, while, according to their localization on the chalcogen atoms, the MOs 18a′ and 16a″ of $[Fe(C_5H_4S)_2S]$ (**1a**) undergo a significant destabilization. In **3c**, the out-of-phase linear combinations of Te lone pairs become the HOMO.

These results may account for the electrochemistry. The HOMO–LUMO gaps were computed to be: **1a**, 2.77 eV; **2b**, 2.65 eV; **3c**, 2.40 eV.

Even if in **3c** solvation processes lower this value to $\Delta E = 1.53$ eV, it is still conceivable that **3c** is particularly accessible to one-electron addition-removal processes.

2.3. *Electrochemistry of the 1,3-ditellura[3]ferrocenophanes $[Fe(C_5H_4Te)_2E']$ (E′ = S, Se or CH_2)*

Figure 5 compares the cyclic voltammetric responses to one-electron oxidation of **3a**, **3b**, **3c** and **3d**.

Substitution of the central bridging tellurium atom (E′) does not modify the electrochemical response appreciably, except for a slight shift towards more positive potentials, consistent with lower electron density. More dramatic effects seem to result from the incorporation of a methylene fragment into the bridging position, in that oxidation is notably favoured, although electron removal is hindered as judged from the peak-to-peak separation.

Similar to $[Fe(C_5H_4Te)_2Te]^+$, the electrogenerated cation $[Fe(C_5H_4Te)_2S]^+$ in polycrystalline powder has no EPR activity at 4 K.

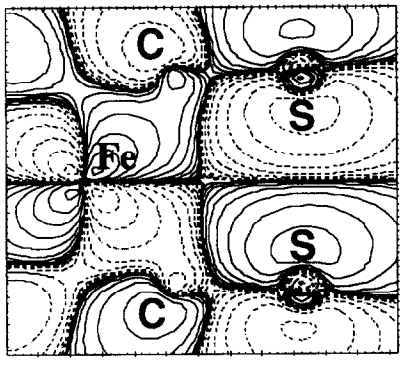

MO 16a" in the XY Plane

Fig. 4. DV-Xα contour plots of the 16a″ MO in the *XY* plane. Logarithmic contour levels are $\pm 8\times10^{-4}$; $\pm 16\times10^{-4}$; $\pm 32\times10^{-4}\ldots e^{1/2}$ Å$^{-3/2}$.

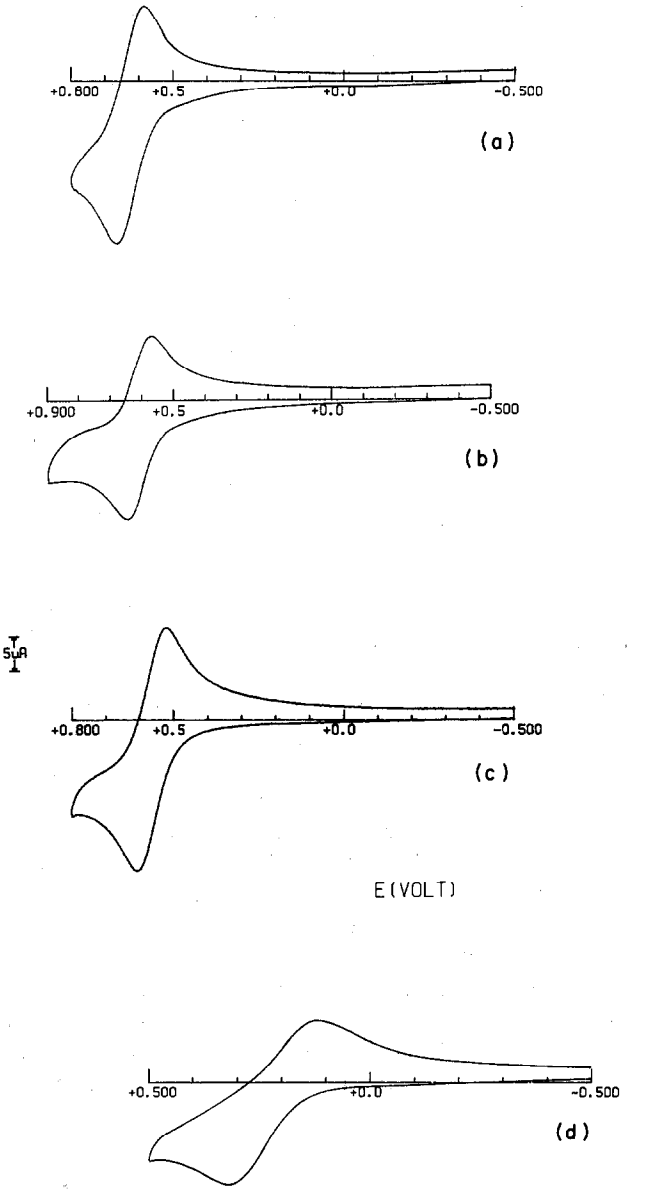

Fig. 5. Cyclic voltammograms recorded at a platinum electrode on CH_2Cl_2 solutions containing $[NBu_4]ClO_4]$ (0.2 mol dm^{-3}) and: (a) $[Fe(C_5H_4Te)_2S]$ (**3a**) (1.1×10^{-3} mol dm^{-3}); (b) $[Fe(C_5H_4Te)_2Se]$ (**3b**) (8.0×10^{-4} mol dm^{-3}); (c) $[Fe(C_5H_4Te)_2Te]$ (**3c**) (1.2×10^{-3} mol dm^{-3}); (d) $[Fe(C_5H_4Te)_2(CH_2)]$ (**3d**) (8.0×10^{-4} mol dm^{-3}). Scan rate 0.2 V/s^{-1}.

TABLE 4. Redox potentials (in V, *vs.* SCE) and peak-to-peak separations (in mV, at 0.1 V/s^{-1}) for the one-electron oxidation of tellura-[3]ferrocenophanes [a] and related chalcogena [3]ferrocenophanes [10–12]

Compound	$E^{\circ\prime}$ (V) [b]	ΔE_p (mV)	Solvent	Reference
1a $Fe(C_5H_4S)_2S$	+0.73		MeCN/THF [c]	10
2b $Fe(C_5H_4Se)_2Se$	+0.64		MeCN/THF [c]	10
3c $Fe(C_5H_4Te)_2Te$	+0.56	70	MeCN/THF [c]	This work
1a $Fe(C_5H_4S)_2S$	+0.68		MeCN	12
1b $Fe(C_5H_4S)_2Se$	+0.64		MeCN	12
	+0.69		MeCN/THF [c]	10
1c $Fe(C_5H_4S)_2Te$	+0.58		MeCN/THF [c]	10
1d $Fe(C_5H_4S)_2CH_2$	+0.59		MeCN	12
2a $Fe(C_5H_4Se)_2S$	+0.63		MeCN	12
2b $Fe(C_5H_4Se)_2Se$	+0.59		MeCN	12
2c $Fe(C_5H_4Se)_2Te$	[d]			
2d $Fe(C_5H_4Se)_2CH_2$	+0.56		MeCN	12
	+0.60		MeCN/THF [c]	10
3a $Fe(C_5H_4Te)_2S$	+0.62	74	CH_2Cl_2	This work
3b $Fe(C_5H_4Te)_2Se$	+0.61	74	CH_2Cl_2	This work
3c $Fe(C_5H_4Te)_2Te$	+0.57	74	CH_2Cl_2	This work
3d $Fe(C_5H_4Te)_2CH_2$	+0.22	175	CH_2Cl_2	This work
$Fe(C_5H_5)_2$	+0.38	70	MeCN	This work
	+0.44	78	CH_2Cl_2	This work

[a] Present work. [b] The redox potentials given in refs. 11 and 12 were converted to values *vs.* SCE. [c] Solvent mixture 1:1 (v/v). [d] Not measured.

Table 4 summarizes the electrochemical data of **3a–3d**, and the literature data for the related thia- and selena-[3]ferrocenophanes [10–12]. The relatively high oxidation potentials of thia[3]ferrocenophanes are progressively lowered if the heavier chalcogens selenium and tellurium, respectively, are introduced into the intramolecular trichalcogen bridge. However, all trichalcogena[3]ferrocenophanes are less easily oxidised than ferrocene itself.

3. Experimental details

The tellura[3]ferrocenophanes were prepared according to reported procedures [2,3].

Anhydrous dichloromethane, acetonitrile and tetrahydrofuran (packaged under dinitrogen, 100 ml bottles) for electrochemistry were Aldrich products. Tetrabutylammonium perchlorate (Fluka) and tetraethylammonium perchlorate (Carlo Erba) supporting electrolytes were commercial products, which were dried and stored in a vacuum oven at 40°C.

The cyclic voltammetric measurements were performed with a BAS 100A electrochemical analyzer. A three electrode cell was designed to allow the tip of the saturated calomel reference electrode (SCE) to approach closely, via a Luggin capillary, the platinum disk working electrode, which in turn was surrounded by a platinum spiral counter-electrode.

Controlled potential coulometry was carried out by using an AMEL-Mod. 552 potentiostat, connected to an AMEL-Mod. 558 integrator. A three-compartment cell was designed with a central unit bearing platinum gauze working macroelectrode. The lateral compartments contained the reference (SCE) and the auxiliary (mercury pool) electrodes, respectively. The compartments containing the working and the auxiliary electrodes were separated by a sintered glass disk.

Deoxygenation of the solutions was by bubbling ultrapure dinitrogen for at least 10 min.

All the potential values are referred to SCE.

4. Calculations

The quantum mechanical calculations have been run with the self-consistent one-electron local density approach. The non-relativistic form of the one-electron Schrödinger equation can be written (in Hartree atomic units, σ represents spin) as

$$H_\sigma \Psi_{i\sigma}(r) = \epsilon_{i\sigma} \Psi_{i\sigma}(r) \quad (1)$$

where

$$H_\sigma = \left[-\tfrac{1}{2}\nabla^2 + V_c(r) + V_{xc,\sigma}(r) \right] \quad (2)$$

The three terms refer to the kinetic energy, the Coulomb potential and the exchange-correlation potential, respectively. As far as the effective single particle exchange-correlation potential is concerned, the Slater $X\alpha$ form [26] (see eqn. (3)) was employed. Throughout the calculations we used $\alpha = 0.7$, which is close to the Kohn–Sham value of 2/3. Variation of α between 2/3 and 0.7 has insignificant effects on our results.

$$V_{xc,\sigma} = -3\alpha \left[\frac{3\rho_\sigma}{4\pi} \right]^{\frac{1}{3}} \quad (3)$$

The matrix elements of the effective Hamiltonian and of the symmetry orbital overlap matrix S were evaluated as discrete sums over a set of sample points. This set includes not only pseudorandom diophantine points [27–29] but also a regular spherical volume mesh which has been added in order to obtain a better accuracy in the description of the wavefunction in the region close to the nuclei.

The occupation numbers of each MO were determined by applying Fermi–Dirac statistics. The Coulomb potential was computed by a one-dimensional integration by replacing the actual electron charge density with a model density, *i.e.* the "true" electron charge density has been cast in a multicentre overlapping multipolar form [30].

An extended basis set has been used for all the atoms (Fe, 1s–4d AOs; Te, 1s–4f–5d AOs; Se, 1s–4d

AOs; S, 1s–3d AOs; C, 1s–3p AOs) with the exclusion of H where a minimal basis set was adopted. Spherical wells (2 Ry deep) having an internal and external radius of 4.0 and 6.0 au, respectively, were added to the atomic potentials. Such a procedure provides a practical means for extending the basis to deal with diffuse orbitals. Moreover, it is flexible enough so that the basis sets can be optimized for the particular molecular application.

The experimental geometry of the title compounds [2] was idealized to C_s symmetry. The calculations have been performed on a DEC5200/CX (Digital Equipments) workstation at the Inorganic Chemistry Department of the University of Padova.

References

1 A. Davison and J. C. Smart, *J. Organomet. Chem., 19* (1969) 7.
2 M. Herberhold, P. Leitner and U. Thewalt, *Z. Naturforsch, 45b* (1990) 1503.
3 M. Herberhold and P. Leitner, *J. Organomet. Chem., 411* (1991) 233.
4 B. R. Davis and I. Bernal, *J. Cryst. Mol. Struct., 2* (1972) 107.
5 A. G. Osborne, R. E. Hollands, J. A. K. Howard and R. F. Bryan, *J. Organomet. Chem., 205* (1981) 395.
6 R. F. Bryan, as quoted in ref. 8.
7 A. J. Blake, R. O. Gould and A. G. Osborne, *J. Organomet. Chem., 308* (1986) 297.
8 E. W. Abel, M. Booth and K. G. Orrell, *J. Organomet. Chem., 208* (1981) 213.
9 E. W. Abel, K. G. Orrell, A. G. Osborne, V. Sik, and Wang Guoxiong, *J. Organomet. Chem., 411* (1991) 239.
10 A. G. Osborne, R. E. Hollands and A. G. Nagy, *J. Organomet. Chem., 373* (1989) 229.
11 H. Ushijima, T. Akiyama, M. Kajitani, K. Shimizu, M. Aoyama, S. Masuda, Y. Harada and A. Sugimori, *Chem. Lett.* (1987) 2197.
12 H. Ushijima, T. Akiyama, M. Kajitani, K. Shimizu, M. Aoyama, S. Masuda, Y. Harada and A. Sugimori, *Bull. Chem. Soc. Jpn., 63* (1990) 1015.
13 E. R. Brown and J. R. Sandifer, in B. W. Rossiter and J. F. Hamilton (eds.), *Physical Methods of Chemistry*: Electrochemical Methods, Vol. 2, Wiley, New York, 1986, Chapter 4.
14 A. Cinquantini, G. Opromolla and P. Zanello, *J. Chem. Soc. Dalton Trans.*, (1991) 3161 and references cited therein.
15 R. Martinez and A. Tiripicchio, *Acta Crystallogr., C46* (1990) 202.
16 J. Pickardt, H. Schumann and R. Mohtachemi, *Acta Crystallogr. C46* (1990) 39.
17 T.-Y. Dong, H.-M. Lin, M.-Y, Hwang, T.-Y. Lee, L.-H. Tseng, S.-M. Peng and G.-H. Lee, *J. Organomet. Chem., 414* (1991) 227.
18 T. Saji and N. Ito, *Bull. Chem. Soc. Jpn., 58* (1985) 3375, and references cited therein.
19 Y. S. Sohn, D. N. Hendrickson and H. B. Gray, *J. Am. Chem. Soc., 93* (1971) 3603.
20 S. Evans, M. L. H. Green, B. Jewitt, A. F. Orchard and C. F. Pygall, *J. Chem. Soc. Faraday Trans. II, 68* (1972) 1847.
21 J. W. Lauher and R. Hoffmann, *J. Am. Chem. Soc., 98* (1976) 1729.
22 C. Furlani and C. Cauletti, *Struct. Bonding (Berlin), 35* (1978) 119, and references cited therein.
23 C. Cauletti, J. C. Green, M. R. Kelly, P. Powell, J. Van Tilborg, J. Robbins and J. Smart, *J. Photoelectron Spectrosc. Relat. Phenom., 19* (1982) 327.
24 G. Cooper, J. C. Green and P. Payne, *Mol. Phys., 63* (1988) 1031.
25 R. S. Mulliken, *J. Chem. Phys., 23* (1955) 1833.
26 J. C. Slater, in *Quantum Theory of Molecules and Solids: The Self-Consistent Field for Molecules and Solids*, Vol. 4, McGraw-Hill, New York, 1974.
27 D. E. Ellis, *Int. J. Quantum Chem., S2* (1968) 35.
28 D. E. Ellis and G. S. Painter, *Phys. Rev. B, 2,* (1970) 2887.
29 C. B. Haselgrove, *Math. Comput., 15* (1961) 323.
30 B. Delley and D. E. Ellis, *J. Chem. Phys., 76* (1982) 1949.